Published OnlineFirst October 21, 2011; DOI:10.1158/1078-0432.CCR-11-0868

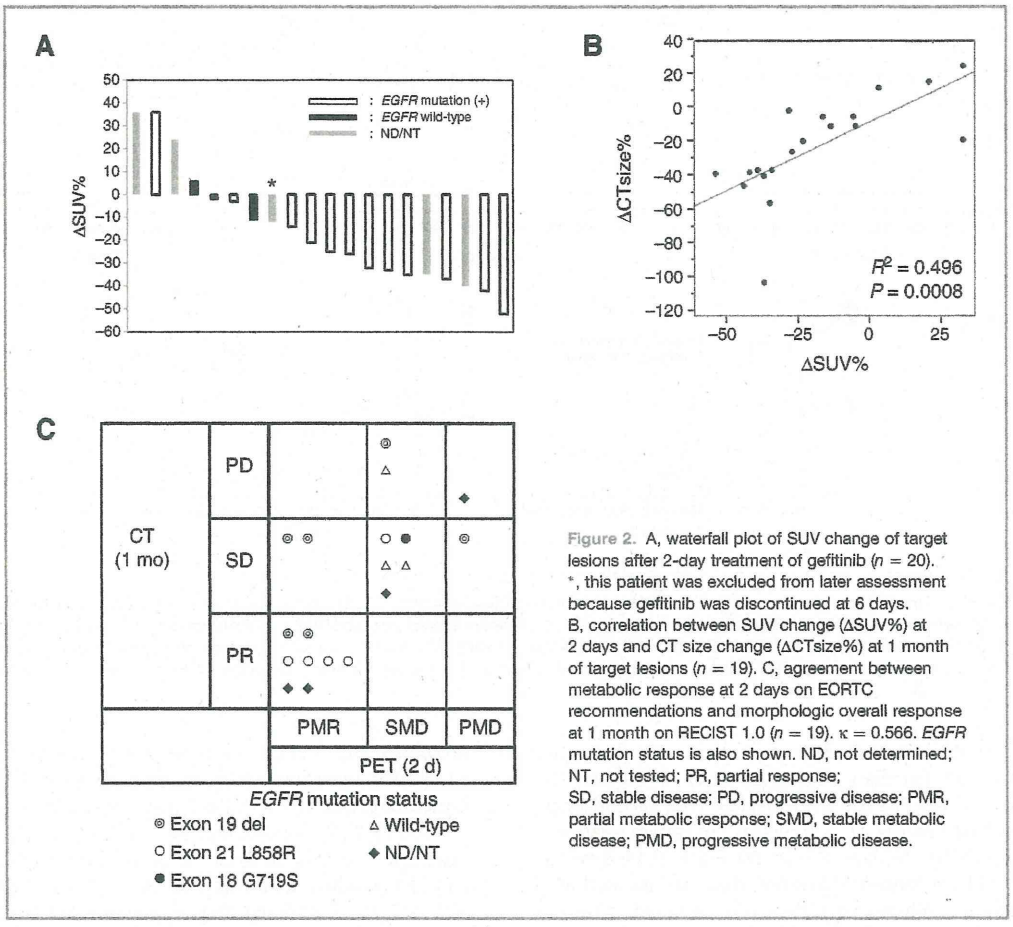

Figure 2. A, waterfall plot of SUV change of target lesions after 2-day treatment of gefitinib ($n = 20$). *, this patient was excluded from later assessment because gefitinib was discontinued at 6 days. B, correlation between SUV change (ΔSUV%) at 2 days and CT size change (ΔCTsize%) at 1 month of target lesions ($n = 19$). C, agreement between metabolic response at 2 days on EORTC recommendations and morphologic overall response at 1 month on RECIST 1.0 ($n = 19$). $\kappa = 0.566$. *EGFR* mutation status is also shown. ND, not determined; NT, not tested; PR, partial response; SD, stable disease; PD, progressive disease; PMR, partial metabolic response; SMD, stable metabolic disease; PMD, progressive metabolic disease.

6 patients had an exon 19 deletion, 5 patients had an exon 21 L858R mutation, and one had an exon 18 G719S mutation. Median ΔSUV% changes of target lesions in patients with mutated *EGFR* and wild-type *EGFR* were −29% and −2%, respectively (Fig. 2A). Of 12 patients with activating *EGFR* mutations, 8 (67%) were metabolic responders and 3 were with stable metabolic disease at 2 days, whereas 6 (50%) were morphologic responders and 5 were morphologically with stable disease at 1 month (Fig. 2C). Conversely, of 8 *EGFR* gene-assessable metabolic responders at 2 days, all had the activating mutations and 6 were assessed as morphologic responders at 1 month. Of 6 *EGFR* gene-assessable morphologic responders at 1 month, all had the mutations and were assessed as metabolic responders at 2 days. An 83-year-old female patient with an exon 19 deletion was assessed as having progressive metabolic disease while being with morphologically stable disease. During follow-up, this patient suffered from a relapse at 48 days. Another 79-year-old female patient with an exon 19 deletion was with stable metabolic disease at 2 days but assessed as having progressive disease because a new lesion appeared on PET/CT images at 1 month. All of 3 patients with wild-type *EGFR* were assessed with metabolically stable disease at 2 days. Two of these were assessed with morphologically stable disease and one had progressive disease at 1 month (Fig. 2C).

PFS according to metabolic and morphologic responses

When a cutoff value of −25% in ΔSUV% was used between metabolic responders and nonresponders, PFS did not significantly correlate with metabolic response at 2 days. Median PFS of the responders and nonresponders was 290 days and 48 days, respectively (log-rank $P = 0.095$; Fig. 3A). This was attributable to a 58-year-old male nonresponder with an L858R mutation who was assessed with 21% decrease of ΔSUV% and experienced the longest PFS of 680 days. When a cutoff value of −20%, which was still within the extent recommended by EORTC (22), was used, this patient was included in responders, and 2-day metabolic responders had significantly prolonged PFS compared with metabolic nonresponders (median, 296 vs. 42 days; $P < 0.0001$; Fig. 3B). When metabolic response was evaluated at 1 month, PFS was also significantly longer in

Published OnlineFirst October 21, 2011; DOI:10.1158/1078-0432.CCR-11-0868

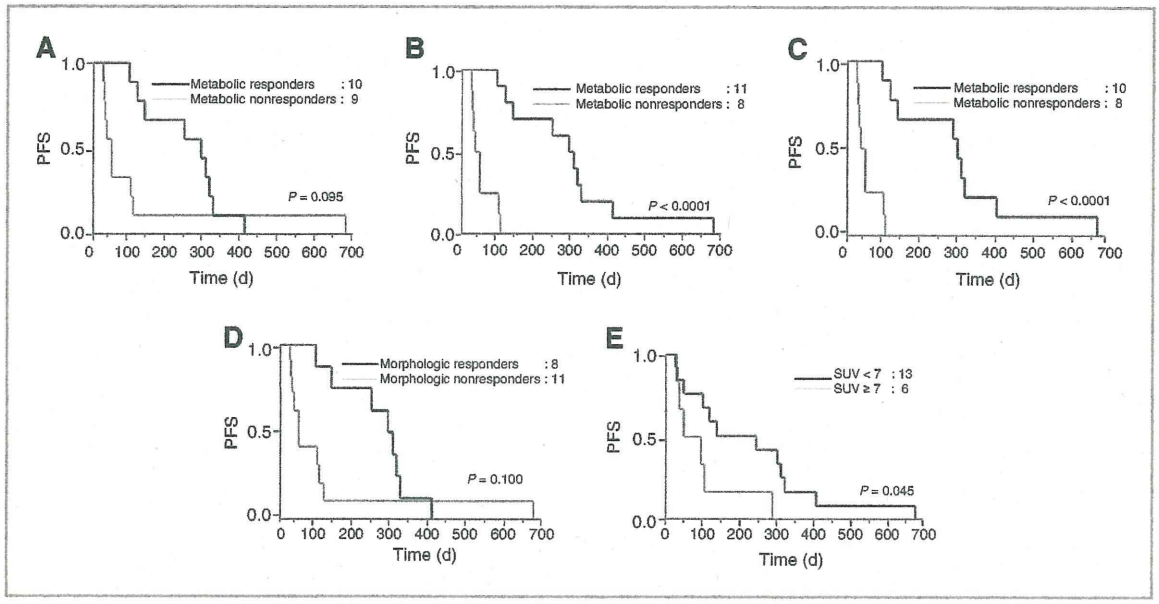

Figure 3. A, PFS of metabolic responders (ΔSUV% < −25%) and nonresponders (ΔSUV% ≥ −25%) at 2 days. B, PFS of metabolic responders (ΔSUV% < −20%) and nonresponders (ΔSUV% ≥ −20%) at 2 days. C, PFS of metabolic responders (ΔSUV% < −25%) and nonresponders (ΔSUV% ≥ −25%) at 1 month. One patient did not have an FDG-PET scan at 1 month, without missing a CT scan. D, PFS of morphologic responders and nonresponders at 1 month. E, PFS according to a single PET activity at 2 days (SUV < 7, black; SUV ≥ 7, gray). *P* values were obtained using the log-rank test.

responders than in nonresponders even with the cutoff value of −25% (median, 302 vs. 42 days; $P < 0.0001$; Fig. 3C). Meanwhile, PFS did not correlate with morphologic response based on RECIST 1.0 even at 1 month of treatment (median, 296 vs. 48 days; $P = 0.100$; Fig. 3D) because the patient with the longest PFS of 680 days was assessed with stable disease. When this patient was excluded, 1-month morphologic response became significantly correlated with PFS ($P = 0.0003$).

In the clinical settings, SUV at baseline PET might be influenced by previous chemotherapy. Therefore, we also investigated whether an early metabolic assessment with a single post-gefitinib PET/CT scan would provide any useful prognostic information. We defined an SUV threshold of 7, which was the nearest integer to the average SUV of the hottest target lesions in PET at 2 days, to separate responders (i.e., SUV < 7) from poor responders (SUV ≥ 7). There was a significant association between post-gefitinib FDG uptake and PFS (median, 244 days with SUV < 7 vs. 71 days with SUV ≥ 7; $P = 0.045$; Fig. 3E). Meanwhile, SUV in baseline PET studies was not predictive of PFS (median, 117 days with SUV < 10 vs. 93 days with SUV ≥ 10; $P = 0.611$).

In univariate analysis using the Cox hazards model, metabolic response using a cutoff value of −20% of ΔSUV% at 2 days was the only predictive factor of PFS (HR = 0.04; $P < 0.0001$), other than *EGFR* mutation status (Table 2).

Table 2. Univariate analysis of predictive factors for PFS

	Analysis		
Predictive factor	***n***	**HR (95% CI)**	***P***
Age (≥70 y)	19	1.69 (0.60–4.58)	0.310
Sex (female)	19	1.19 (0.37–5.29)	0.789
Smoking history (never)	19	1.22 (0.39–5.46)	0.747
Metabolic response at 2 d[a] (yes)	19	0.04 (0.002–0.23)	<0.0001
Morphologic response at 1 mo (yes)	19	0.44 (0.16–1.20)	0.109
EGFR mutation (yes)	15	0.17 (0.03–0.92)	0.041

[a]A cutoff value of −20% in SUV decline was used.

Published OnlineFirst October 21, 2011; DOI:10.1158/1078-0432.CCR-11-0868

In multivariate analysis including metabolic response at 2 days, morphologic response at 1 month, and smoking history, metabolic response at 2 days was the only statistically significant factor ($P = 0.0007$).

OS according to metabolic and morphologic responses

OS did not differ significantly between any metabolic responders and nonresponders and between the morphologic responders and nonresponders (Supplementary Fig. S1), although there was a trend for longer survival in metabolic responders who showed post-gefitinib SUV < 7 at 2 days ($P = 0.066$; Supplementary Fig. S1E).

Discussion

It has been evident that EGFR TKIs, gefitinib and erlotinib, induce dramatic responses in a subpopulation of patients with adenocarcinoma. Although the presence of somatic mutations in the *EGFR* gene is considered to be the best predictor of response to these TKIs (9, 10, 25, 26), its efficacy as biomarker is not satisfactory due to technical problems on biopsy, secondary mutation acquiring the resistance to the EGFR TKIs, and recent data showing response of patients with wild-type *EGFR* to erlotinib (27). Thus, an alternative approach optimizing clinical outcome of EGFR TKI therapy is necessary to accurately select patients who will benefit from the therapy and to avoid critical adverse effects such as interstitial lung disease (28).

Early response to therapy assessed by [^{18}F]FDG-PET has been increasingly established as a prognostic biomarker in various malignancies (13). In NSCLC, two studies have just been published to show that early [^{18}F]FDG-PET evaluation can predict PFS and OS in patients treated with erlotinib (29, 30). Another recent study reported that early [^{18}F]FDG-PET predicted histopathologic response in patients with NSCLC treated with erlotinib as neoadjuvant therapy (31). Metabolic tumor responses were assessed 1 to 8 weeks after the start of erlotinib treatment in these studies. Meanwhile, Su and colleagues showed that gefitinib treatment induced rapid decreases of FDG uptake within 48 hours in sensitive tumors using a mouse model, providing a rationale for earlier assessment in clinical settings (16). In these sensitive tumors, glucose transporters rapidly translocated from the plasma membrane to the cytosol, and reduction of hexokinase activity was observed prior to changes in cell-cycle distribution, thymidine uptake, and apoptosis. Such changes were not found in an early decline of FDG uptake in response to conventional cytotoxic chemotherapy (32). A more recent study preliminarily analyzed 5 patients with advanced NSCLC and reported that, only 2 days after initiation of gefitinib therapy, SUV decreased by a mean of 61% in patients who showed partial response by conventional CT evaluation 4 weeks later (17).

Consistent with these studies, SUV decreased by up to a maximum of 52% at 2 days in the present prospective study, and we observed a strong correlation between changes in SUV at 2 days and those in tumor size at 1 month. There was also a moderate agreement between metabolic responses at 2 days based on the EORTC recommendations and morphologic responses at 1 month according to RECIST 1.0. Moreover, metabolic response at 2 days could be a predictor of prolonged PFS when a cutoff value of −20% in SUV decline was used. The cutoff value of −25%, which was used in several other studies (33–35) but did not reach statistical significance in the present study, might be too large for the evaluation only after 2 days and for the sample size as small as 20. A single PET study at 2 days might also provide prognostic information. Patients with favorable response with lower post-gefitinib SUVs (SUV < 7) revealed longer PFS than poorly responding patients with higher SUVs (SUV ≥ 7), although significance was weak. There was a trend for an association between morphologic response at 1 month and improved PFS but it did not reach statistical significance, due to the presence of an *EGFR* mutation-positive patient showing stable disease but with a long PFS. In terms of OS, there was not significant difference, probably due to the small sample size and because OS is influenced by the second-line or later treatment. Together, although our study was a single-centered with a small number of patients, we propose that assessment of FDG uptake at 2 days could be a superior predictor of post-gefitinib outcome to conventional CT evaluation in its accuracy and rapidity.

Of 12 patients with activating *EGFR* mutations, 10 (83%) showed partial response or were with stable disease both in FDG-PET at 2 days and CT evaluation at 1 month. Thus, mutated *EGFR* is a good biomarker for response to gefitinib, as previously reported (6). Exceptionally, an 83-year-old female patient with exon 19 deletion had progressive metabolic disease at 2 days while being with morphologically stable disease at 1 month. She had a PFS of 48 days and this was relatively short for morphologically stable disease, the median PFS of which was 100 days. Another 79-year-old female patient with exon 19 deletion was with stable metabolic disease at 2 days while having morphologically progressive disease at 1 month. Her PFS was 30 days and relatively short for stable metabolic disease, the median PFS of which was 48 days. Thus, there was still inconsistency among *EGFR* mutations, early FDG-PET evaluation, or conventional CT evaluation, and larger prospective studies will be needed to clarify which is the best predictor of survival. Meanwhile, although it appears reasonable that none of 3 patients with wild-type *EGFR* showed metabolic or morphologic response, the number of patients is too small to discuss more about wild-type *EGFR*.

Interstitial lung disease is the most severe adverse effect, which occurs in approximately 1% of EGFR TKI–treated patients worldwide. Onset of symptoms may begin only after 2 days of gefitinib therapy. Median onset was 24 days in Japan and 42 days in United States, and about 1 of 3 of the cases were fatal (28). It has been suggested that [^{18}F]FDG-PET may help to evaluate interstitial lung disease. Positive FDG uptake was observed in 86% of patients with idiopathic pulmonary fibrosis and correlated with disease

Published OnlineFirst October 21, 2011; DOI:10.1158/1078-0432.CCR-11-0868

activity (36). In the present study, a 77-year-old male patient showed ground-glass opacity suggestive of interstitial infiltrate on chest radiograph, and gefitinib was discontinued at 6 days of treatment. At 2 days of treatment, his PET images did not show any positive uptake in lung parenchyma, and later on a CT scan, this infiltrate was rather considered a secondary change associated with obstructive bronchus. No other patient presented with interstitial infiltrate on chest radiograph. Thus, we could not determine at the moment whether [^{18}F]FDG-PET can early detect gefitinib-induced lung damage.

In summary, early response assessment by FDG-PET could help to identify patients with lung adenocarcinoma who will benefit from gefitinib treatment. The present study showed promising data suggesting that clinical outcome can be predicted only after 2 days of the treatment. This early assessment may allow for rapid initiation of alternative strategies and minimize critical adverse effects such as interstitial lung disease when gefitinib is ineffective. The main limitation is the small sample size, and validation with prospective studies in a larger patient population is warranted.

Disclosure of Potential Conflicts of Interest

No potential conflicts of interest were disclosed.

Acknowledgments

The authors thank Y. Habe for secretarial assistance.

Grant Support

The work was supported by the grand-in-aid for community health and medical care from the Osaka University Medical School Alumni and the award from the Osaka Cancer Association. This trial is registered at www.umin.ac.jp/ctr/index/htm as UMIN000003621.

The costs of publication of this article were defrayed in part by the payment of page charges. This article must therefore be hereby marked *advertisement* in accordance with 18 U.S.C. Section 1734 solely to indicate this fact.

Received April 14, 2011; revised October 6, 2011; accepted October 9, 2011; published OnlineFirst October 21, 2011.

References

1. Sharma SV, Bell DW, Settleman J, Haber DA. Epidermal growth factor receptor mutations in lung cancer. Nat Rev Cancer 2007;7:169–81.
2. Fukuoka M, Yano S, Giaccone G, Tamura T, Nakagawa K, Douillard JY, et al. Multi-institutional randomized phase II trial of gefitinib for previously treated patients with advanced non-small-cell lung cancer (The IDEAL 1 Trial) [corrected]. J Clin Oncol 2003;21:2237–46.
3. Kris MG, Natale RB, Herbst RS, Lynch TJ Jr, Prager D, Belani CP, et al. Efficacy of gefitinib, an inhibitor of the epidermal growth factor receptor tyrosine kinase, in symptomatic patients with non-small cell lung cancer: a randomized trial. JAMA 2003;290:2149–58.
4. Shepherd FA, Rodrigues Pereira J, Ciuleanu T, Tan EH, Hirsh V, Thongprasert S, et al. Erlotinib in previously treated non-small-cell lung cancer. N Engl J Med 2005;353:123–32.
5. Thatcher N, Chang A, Parikh P, Rodrigues Pereira J, Ciuleanu T, von Pawel J, et al. Gefitinib plus best supportive care in previously treated patients with refractory advanced non-small-cell lung cancer: results from a randomised, placebo-controlled, multicentre study (Iressa Survival Evaluation in Lung Cancer). Lancet 2005;366:1527–37.
6. Gazdar AF. Activating and resistance mutations of EGFR in non-small-cell lung cancer: role in clinical response to EGFR tyrosine kinase inhibitors. Oncogene 2009;28 Suppl 1:S24–31.
7. Hirsch FR, Varella-Garcia M, Cappuzzo F. Predictive value of EGFR and HER2 overexpression in advanced non-small-cell lung cancer. Oncogene 2009;28 Suppl 1:S32–7.
8. Mok TS, Wu YL, Thongprasert S, Yang CH, Chu DT, Saijo N, et al. Gefitinib or carboplatin-paclitaxel in pulmonary adenocarcinoma. N Engl J Med 2009;361:947–57.
9. Maemondo M, Inoue A, Kobayashi K, Sugawara S, Oizumi S, Isobe H, et al. Gefitinib or chemotherapy for non-small-cell lung cancer with mutated EGFR. N Engl J Med 2010;362:2380–8.
10. Mitsudomi T, Morita S, Yatabe Y, Negoro S, Okamoto I, Tsurutani J, et al. Gefitinib versus cisplatin plus docetaxel in patients with non-small-cell lung cancer harbouring mutations of the epidermal growth factor receptor (WJTOG3405): an open label, randomised phase 3 trial. Lancet Oncol 2010;11:121–8.
11. John T, Liu G, Tsao MS. Overview of molecular testing in non-small-cell lung cancer: mutational analysis, gene copy number, protein expression and other biomarkers of EGFR for the prediction of response to tyrosine kinase inhibitors. Oncogene 2009;28 Suppl 1:S14–23.
12. Burris HA III. Shortcomings of current therapies for non-small-cell lung cancer: unmet medical needs. Oncogene 2009;28 Suppl 1:S4–13.
13. Vansteenkiste J, Fischer BM, Dooms C, Mortensen J. Positron-emission tomography in prognostic and therapeutic assessment of lung cancer: systematic review. Lancet Oncol 2004;5:531–40.
14. Stroobants S, Goeminne J, Seegers M, Dimitrijevic S, Dupont P, Nuyts J, et al. 18FDG-Positron emission tomography for the early prediction of response in advanced soft tissue sarcoma treated with imatinib mesylate (Glivec). Eur J Cancer 2003;39:2012–20.
15. Jager PL, Gietema JA, van der Graaf WT. Imatinib mesylate for the treatment of gastrointestinal stromal tumours: best monitored with FDG PET. Nucl Med Commun 2004;25:433–8.
16. Su H, Bodenstein C, Dumont RA, Seimbille Y, Dubinett S, Phelps ME, et al. Monitoring tumor glucose utilization by positron emission tomography for the prediction of treatment response to epidermal growth factor receptor kinase inhibitors. Clin Cancer Res 2006;12:5659–67.
17. Sunaga N, Oriuchi N, Kaira K, Yanagitani N, Tomizawa Y, Hisada T, et al. Usefulness of FDG-PET for early prediction of the response to gefitinib in non-small cell lung cancer. Lung Cancer 2008;59:203–10.
18. Nagai Y, Miyazawa H, Huqun, Tanaka T, Udagawa K, Kato M, et al. Genetic heterogeneity of the epidermal growth factor receptor in non-small cell lung cancer cell lines revealed by a rapid and sensitive detection system, the peptide nucleic acid-locked nucleic acid PCR clamp. Cancer Res 2005;65:7276–82.
19. Inohara H, Enomoto K, Tomiyama Y, Higuchi I, Inoue T, Hatazawa J. Impact of FDG-PET on prediction of clinical outcome after concurrent chemoradiotherapy in hypopharyngeal carcinoma. Mol Imaging Biol 2010;12:89–97.
20. Therasse P, Arbuck SG, Eisenhauer EA, Wanders J, Kaplan RS, Rubinstein L, et al. New guidelines to evaluate the response to treatment in solid tumors. European Organization for Research and Treatment of Cancer, National Cancer Institute of the United States, National Cancer Institute of Canada. J Natl Cancer Inst 2000;92:205–16.
21. Antoch G, Kanja J, Bauer S, Kuehl H, Renzing-Koehler K, Schuette J, et al. Comparison of PET, CT, and dual-modality PET/CT imaging for monitoring of imatinib (STI571) therapy in patients with gastrointestinal stromal tumors. J Nucl Med 2004;45:357–65.
22. Young H, Baum R, Cremerius U, Herholz K, Hoekstra O, Lammertsma AA, et al. Measurement of clinical and subclinical tumour response using [18F]-fluorodeoxyglucose and positron emission tomography: review and 1999 EORTC recommendations. European Organization for Research and Treatment of Cancer (EORTC) PET Study Group. Eur J Cancer 1999;35:1773–82.

Published OnlineFirst October 21, 2011; DOI:10.1158/1078-0432.CCR-11-0868

23. Svanholm H, Starklint H, Gundersen HJ, Fabricius J, Barlebo H, Olsen S. Reproducibility of histomorphologic diagnoses with special reference to the kappa statistic. APMIS 1989;97:689–98.
24. Lee ET, Go OT. Survival analysis in public health research. Annu Rev Public Health 1997;18:105–34.
25. Paez JG, Janne PA, Lee JC, Tracy S, Greulich H, Gabriel S, et al. EGFR mutations in lung cancer: correlation with clinical response to gefitinib therapy. Science 2004;304:1497–500.
26. Lynch TJ, Bell DW, Sordella R, Gurubhagavatula S, Okimoto RA, Brannigan BW, et al. Activating mutations in the epidermal growth factor receptor underlying responsiveness of non-small-cell lung cancer to gefitinib. N Engl J Med 2004;350:2129–39.
27. Cappuzzo F, Ciuleanu T, Stelmakh L, Cicenas S, Szczesna A, Juhasz E, et al. Erlotinib as maintenance treatment in advanced non-small-cell lung cancer: a multicentre, randomised, placebo-controlled phase 3 study. Lancet Oncol 2010;11:521–9.
28. Cersosimo RJ. Gefitinib: an adverse effects profile. Expert Opin Drug Saf 2006;5:469–79.
29. Zander T, Scheffler M, Nogova L, Kobe C, Engel-Riedel W, Hellmich M, et al. Early prediction of nonprogression in advanced non-small-cell lung cancer treated with erlotinib by using [(18)F]fluorodeoxyglucose and [(18)F]fluorothymidine positron emission tomography. J Clin Oncol 2011;29:1701–8.
30. Mileshkin L, Hicks RJ, Hughes BG, Mitchell PL, Charu V, Gitlitz BJ, et al. Changes in 18F-fluorodeoxyglucose and 18F-fluorodeoxythymidine positron emission tomography imaging in patients with non-small cell lung cancer treated with erlotinib. Clin Cancer Res 2011; 17:3304–15.
31. Aukema TS, Kappers I, Olmos RA, Codrington HE, van Tinteren H, van Pel R, et al. Is 18F-FDG PET/CT useful for the early prediction of histopathologic response to neoadjuvant erlotinib in patients with non-small cell lung cancer? J Nucl Med 2010;51:1344–8.
32. Shields AF, Mankoff DA, Link JM, Graham MM, Eary JF, Kozawa SM, et al. Carbon-11-thymidine and FDG to measure therapy response. J Nucl Med 1998;39:1757–62.
33. Goerres GW, Stupp R, Barghouth G, Hany TF, Pestalozzi B, Dizendorf E, et al. The value of PET, CT and in-line PET/CT in patients with gastrointestinal stromal tumours: long-term outcome of treatment with imatinib mesylate. Eur J Nucl Med Mol Imaging 2005;32:153–62.
34. Prior JO, Montemurro M, Orcurto MV, Michielin O, Luthi F, Benhattar J, et al. Early prediction of response to sunitinib after imatinib failure by 18F-fluorodeoxyglucose positron emission tomography in patients with gastrointestinal stromal tumor. J Clin Oncol 2009;27:439–45.
35. Lee DH, Kim SK, Lee HY, Lee SY, Park SH, Kim HY, et al. Early prediction of response to first-line therapy using integrated 18F-FDG PET/CT for patients with advanced/metastatic non-small cell lung cancer. J Thorac Oncol 2009;4:816–21.
36. Meissner HH, Soo Hoo GW, Khonsary SA, Mandelkern M, Brown CV, Santiago SM. Idiopathic pulmonary fibrosis: evaluation with positron emission tomography. Respiration 2006;73:197–202.

Epithelial to Mesenchymal Transition Is a Determinant of Sensitivity to Chemoradiotherapy in Non-Small Cell Lung Cancer

Yasushi Shintani, MD, PhD, Akira Okimura, DDS, PhD, Katsutoshi Sato, PhD, Tomoyuki Nakagiri, MD, PhD, Yoshihisa Kadota, MD, PhD, Masayohi Inoue, MD, PhD, Noriyoshi Sawabata, MD, PhD, Masato Minami, MD, PhD, Naoki Ikeda, MD, PhD, Kunimistu Kawahara, MD, PhD, Tomoshige Matsumoto, MD, PhD, Nariaki Matsuura, MD, PhD, Mitsunori Ohta, MD, PhD, and Meinoshin Okumura, MD, PhD

Department of General Thoracic Surgery, Osaka University Graduate School of Medicine, Osaka; Departments of General Thoracic Surgery, Pathology, and Clinical Research, and Development, Osaka Prefectural Medical Center for Respiratory and Allergic Disease, Osaka; and Department of Molecular Pathology, Graduate School of Medicine and Health Sciences, Osaka University, Suita, Osaka, Japan

Background. The epithelial to mesenchymal transition (EMT) is a fundamental biological process during which epithelial cells change to a mesenchymal phenotype; it has a profound impact on cancer progression. The purpose of this study was to clarify the role of EMT in the sensitivity of non-small cell lung cancer (NSCLC) to chemoradiotherapy (CRT).

Methods. We evaluated the correlation between EMT and sensitivity to chemotherapy or radiotherapy using NSCLC cells induced to undergo EMT with epidermal growth factor or transforming growth factor-β1. Immunohistochemistry was used to examine the expression of EMT markers, E-cadherin, cytokeratin, N-cadherin, and vimentin in 50 tumor specimens obtained from patients with NSCLC both before and after CRT.

Results. The EMT resulted in increased malignant potential and reduced sensitivity to cisplatin and paclitaxel in NSCLC cells. Furthermore, chronic exposure to cisplatin, paclitaxel, or radiation altered the cells into therapy-resistant sub-lines that showed phenotypic changes such as a spindle-cell shape and increased EMT marker expression. Also, decreased expression of epithelial markers and upregulation of mesenchymal markers were detected in surgically resected specimens after CRT compared with biopsy specimens obtained before treatment. The disease-free survival rate of patients with EMT marker-positive tumors was significantly lower than that of those with EMT marker-negative tumors.

Conclusions. The EMT marker expression was detected in NSCLC tumors after CRT, indicating that EMT changes are associated with insensitivity to CRT. New therapeutic combinations using EMT-signaling inhibitors may be needed to circumvent the resistance of some types of cancer to CRT.

(Ann Thorac Surg 2011;92:1794–1804)

The results of surgical resection alone for locally advanced non-small cell lung cancer (NSCLC) are poor, and thus the option of induction chemoradiotherapy (CRT) has been developed [1–3]. Although there is consensus about the indication for a multimodal approach in most patients with locally advanced disease, there is no clear agreement about which local therapy should be applied in any given situation [4]. Another continuing problem in the management of lung cancer is metastatic disease, which indicates the importance of gaining a better understanding of biological changes that promote the aggressive neoplastic phenotype [5].

The epithelial to mesenchymal transition (EMT) is a fundamental biological process during which epithelial cells lose their polarity and change to a mesenchymal phenotype [6]. Hallmarks of EMT include loss of cell-cell adhesion, reorganization of the actin cytoskeleton, and acquisition of increased migratory characteristics [7]. When cancer cells invade adjacent tissues or metastasize, they use a mechanism similar to EMT [8]. E-cadherin is a transmembrane glycoprotein that mediates cell-cell adhesion and maintains the normal polarized epithelial phenotype, and functions as a tumor suppressor [9, 10]. Many studies have shown that expression of an inappropriate mesenchymal cadherin in epithelial cells is another means by which tumor cells alter their adhesive function [11, 12]. Thus it has been proposed that increased expressions of EMT markers,

Accepted for publication July 15, 2011.

Presented at the Forty-seventh Annual Meeting of The Society of Thoracic Surgeons, San Diego, CA, Jan 31–Feb 2, 2011.

Address correspondence to Dr Shintani, Department of General Thoracic Surgery, Osaka University Graduate School of Medicine, 2-2-L5 Yamadaoka, Suita-city, Osaka 565-0871, Japan; e-mail: yshintani@thoracic.med.osaka-u.ac.jp.

Published by Elsevier Inc

0003-4975/$36.00
doi:10.1016/j.athoracsur.2011.07.032

loss of epithelial markers such as E-cadherin and cytokeratin, and altered expressions of mesenchymal markers such as N-cadherin and vimentin are associated with poor prognosis in NSCLC cases [13–15].

A few recent studies have reported roles for EMT in the chemoresistance of cancer cells to anti-NSCLC agents [16–18]. Some investigators have reported that the EMT process is resistant to apoptosis [19]. Autocrine production of transforming growth factor-beta (TGF-β) confers resistance to apoptosis after an epithelial-mesenchymal transition process in hepatocytes; the role of EGF receptor ligands. We previously reported that the EMT process increases survival signaling through a phosphatidylinositol 3′-kinase to extracellular signal-regulated kinases pathway [20]. Thus we hypothesized that EMT might alter NSCLC tumors and make them insensitive to chemoradiotherapy. To identify new targets for prevention of metastasis, it is important to understand the molecular mechanisms that drive EMT. In the present study, we evaluated the correlation between EMT and sensitivity to chemotherapy or radiotherapy using epidermal growth factor (EGF) or TGF-β1 to induce EMT in NSCLC cells. In addition, we investigated whether EMT was related to acquired resistance to clinical CRT treatment by evaluating tissue samples obtained from patients with NSCLC before and after CRT.

Material and Methods

Reagents, Antibodies, and Cultured Cells

The A549 cells were purchased from American Type Culture Collection (ATCC, Manassas, VA) and maintained in RPMI (Roswell Park Memorial Institute) medium with 10% fetal bovine serum. Antibodies and other reagents used in this study are shown in Appendix 1. Immunofluorescence microscopy and trans-well motility assays were performed as previously described [12].

Real-Time Polymerase Chain Reaction (RT-PCR)

Real-time PCR using TaqMan assays (Applied Biosystems, Carlsbad, CA) was performed using a CFX96 system (BioRad, Hercules, CA). Threshold cycle (Ct) values were determined from triplicate reactions for the test and reference samples of each target and the internal control gene (GAPDH [glyceraldehyde-3-phosphate dehydrogenase]). Relative expression levels were calculated as 2-ΔΔCt.

Cell Viability and Clonogenic Assay

The MTT assays were used to assess cell viability according to the manufacturer's protocol (Roche Applied Science, Mannheim, Germany). Each experiment was performed using 6 replicate wells and 3 independent experiments. The IC_{50} was defined as the drug concentration required to produce a 50% reduction of the optimal density in each test. For the clonogenic assay, 1,000 cells were plated at equal density in 100-mm culture dishes and cultured with or without the indicated reagents for 14 days. The cells were stained with 0.25% crystal violet for 5 minutes and the number of colonies was counted manually. All experiments were performed in triplicate.

Establishment of Treatment-Resistant Cell Lines

Treatment-resistant cell lines were generated from parental cells by continuous exposure to the drugs according to the methods described by Bertolini and colleagues [21]. Briefly, cells were exposed to 30-μM cisplatin or 2-μM paclitaxel in RPMI media, and surviving cells were continuously exposed to increasing dosages and maintained in the culture media at concentrations of 60 μM and 5 μM. To create a radiation-resistant cell line, A549 cells were treated with radiation at 2 Gy per week for a total dose of 60 Gy. A 4-MV X-ray device, obtained from the linear accelerator at Osaka University Graduate School of Medicine, was used to deliver a dose rate of 1.8 Gy per minute. Some cell sub-lines were cloned using a limited dilution method and resistance to radiation was confirmed by further radiation treatment.

Study Population

Sixty-three patients underwent preoperative concurrent CRT and pulmonary resection between 1995 and 2005 at the Osaka Prefectural Medical Center for Respiratory and Allergic Disease, and Osaka University Hospital. An Institutional Review Board approved this retrospective study and written informed consent for surgical intervention was obtained from each patient. Each patient received 2 cycles of cisplatin-vinca alkaloid or cisplatindocetaxel-based chemotherapy every 4 weeks: cisplatin at 80 mg/m^2 on day 1, and vindesine at 3 mg/m^2 on days 1 and 8, with or without mitomycin at 8 mg/m^2 on day 1 [PV(M) regimen]; cisplatin at 80 mg/m^2 on day 1 and vinorelbine at 20 mg/m^2 on days 1 and 8 (nPV regimen); cisplatin at 80 mg/m^2 on day 1 and docetaxel at 60 mg/m^2 on day 1 (DP regimen). Radiotherapy directed at the tumor and mediastinal nodes was started on day 2 at doses greater than 40 Gy and was performed concurrently during cycle 1. A thoracotomy was performed 6 to 8 weeks after completion of CRT and all patients were performed complete resections.

Immunohistochemistry

A primary antibody reaction was performed using antibodies listed in Appendix 1, then incubated overnight at 4°C. The EnVision+ anti-mouse/HRP polymer (DAKO, Carpinteria, CA) was applied and peroxidase activity was visualized with a diaminobenzidine tetrahydrochloride solution. The slides were examined separately by 2 independent pathologists (A.O. and K.K.) unaware of the clinical characteristics of the patients. All sections were scored in a semiquantitative manner according to the modified method described previously by McCarty and colleagues [22] which reflects both the intensity and percentage of cells. Intensity (I) was classified as 0 (no staining), +1 (weak staining), +2 (distinct staining), or +3 (very strong staining). Tumor cells were counted in three ×200 fields and the per-

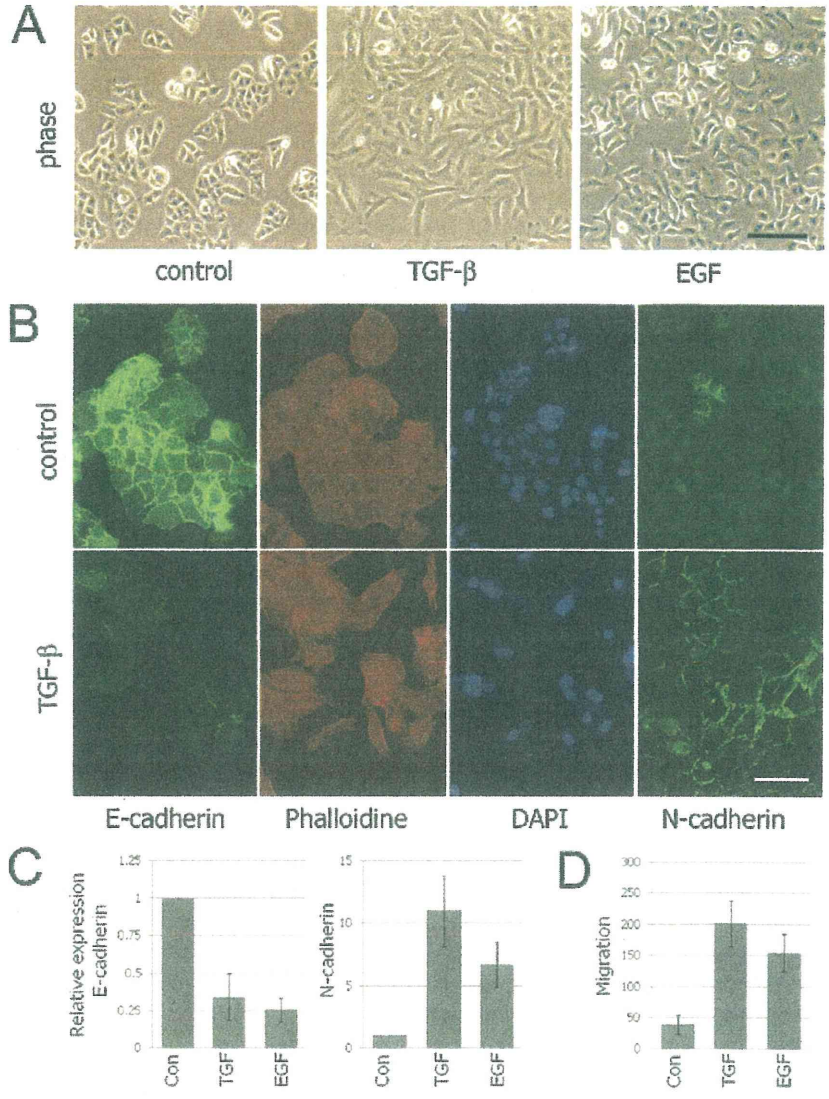

Fig 1. (A) The A549 cells were treated with PBS (as a control), TGF-β1 (2 ng/mL), and EGF (100 ng/mL) for 2 days. Phase contrast images were obtained using a 4.2× objective lens. Bar = 100 μm. (B) The A549 cells were stained for E-cadherin, N-cadherin, 4′,6-diamidino-2-phenylindole, and phalloidine after treatment with PBS (as a control) or TGF-β1 (2 ng/mL). Photographs were obtained using a 40× objective lens. Bar = 50 μm. (C) A549 cells were treated with PBS (control), TGF-β1 (2 ng/mL), or EGF (100 ng/mL) for 1 day, RT-PCR performed to detect E-cadherin and N-cadherin. (D) Motility assays were performed and cells traversing the filter were counted. Columns represent mean values, and bars the standard deviation ($p < 0.05$; control versus TGF or EGF). (con = control; EGF = epidermal growth factor; PBS = phosphate buffered saline; RT-PCR = real-time polymerase chain reaction; TGF = transforming growth factor.)

centage of carcinoma cells with positive staining for each marker was scored. The staining score was calculated for each slide by using the following algorithm: Staining grade (SG) = Σ (I × percentage of carcinoma cells) and the SG was classified as 0 (score<10), +1 (10≤, <30), +2 (30≤, <70), or +3 (70≤).

Statistical Design and Data Analysis

A χ^2 test or Mann-Whitney *U* test was used to compare the results. The disease-free survival (DFS) rates were compared with the results of a log-rank test. The DFS was defined as the time between the date of pulmonary resection and the date of recurrent disease. All patient characteristics were tested against DFS using a Cox-regression analysis based on the tested variable. All statistical analyses were performed using Statview version 5.0 for Windows (Abacus Concepts, Berkeley, CA). A *p* value of less than 0.05 was considered to be statistically significant.

Results

EMT-Induced NSCLC Cells Resistant to Treatment

The TGF-β and EGF both induced EMT in A549 cells, which became more scattered and spindle shaped (Fig 1A). The immunofluorescence (IF) and RT-PCR analysis showed that the expression of E-cadherin decreased, while that of N-cadherin and vimentin increased in EMT-induced cells (Fig 1B, C). In addition, our migration assay findings showed an increased number of cells after EMT induction (Fig 1D), indicating increased malignancy potential.

To determine whether EMT induction resulted in reduced sensitivity to chemotherapy agents such as cisplatin and paclitaxel, we treated the cells with various concentrations of these agents for 2 days after inducing EMT with TGF-β or EGF. The EMT-induced cells showed a significant increase in cell viability in response to cisplatin or paclitaxel compared with untreated control

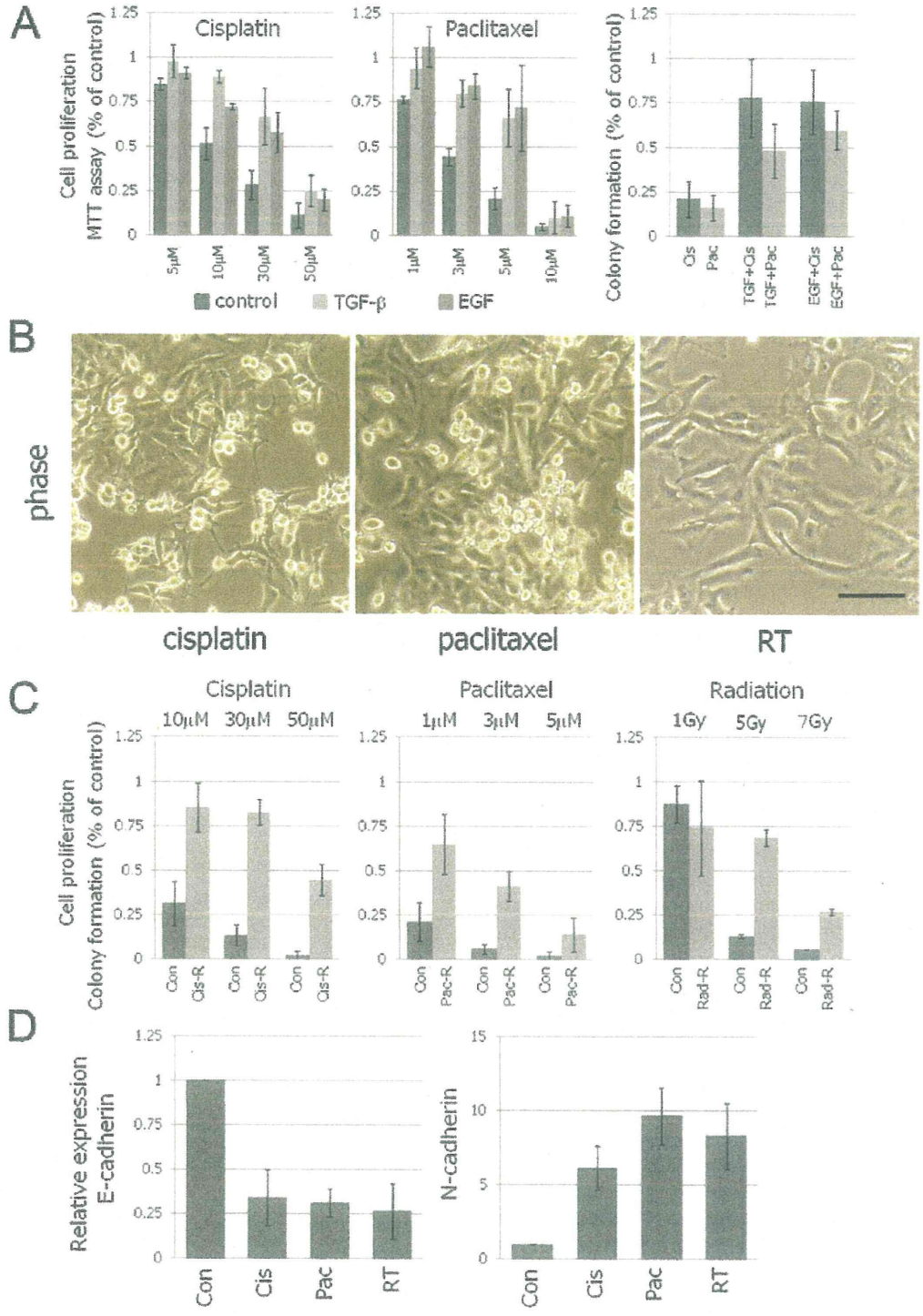

Fig 2. (A) The A549 cells were treated with cisplatin or paclitaxel after inducing EMT using TGF-β (2 ng/mL) or EGF (100 ng/mL). Proliferation of cells was quantified with MTT and clonogenic assays as described in the Material and Methods section; Cis, cisplatin (30 μM); Pac, paclitaxel (5 μM). The EMT-induced cells showed a significant increase in cell viability in response to cisplatin or paclitaxel. (B) Stable treatment-resistant phenotypes were generated by chronic exposure of A549 cells to cisplatin, paclitaxel, and radiation as described in the protocol noted in Materials and Methods section. Phase contrast images were obtained using a 4.2× objective lens. Bar = 100 μm. (C) Proliferation of resistant sub-lines was quantified with a clonogenic assay. (Con = untreated; Cis-R = cisplatin resistant; Pac-R = paclitaxel resistant; Rad-R = radiation-resistant sub-lines). Stable treatment-resistant phenotypes showed improved clonogenic survival in each resistant sub-line. (D) Total RNA was extracted from each resistant sub-line (Con = untreated; Cis = cisplatin resistant; Pac = paclitaxel resistant; RT, = radiation resistant), and real-time polymerase chain reaction was performed for E-cadherin, N-cadherin, and GAPDH (glyceraldehyde-3-phosphate dehydrogenase; as an internal control). (EMT = epithelial to mesenchymal transition; TGF = transforming growth factor.)

Ann Thorac Surg
2011;92:1794–1804

Table 1. The IC_{50} Values (Relative Resistance Ratio) for Cell Lines Against Ciplatin and Paclitaxel[a]

Cell Lines	Cisplatin (μM)	Paclitaxel (μM)
Parent A549 cells	33.2	2.9
A549 treated with TGF-β	62.8 (1.9)	5.8 (2.0)
A549 treated with EGF	55.0 (1.7)	5.5 (1.9)
Cisplatin-resistant cells	142 (4.3)	
Paclitaxel-resistant cells	22.1 (7.6)	

[a] Drug sensitivity was determined by MTT assay as described in Material and Methods. The relative resistance ratio was defined as IC_{50} of the resistant sub-line/IC_{50} of the parent cell line.

EGF = epidermal growth factor; IC_{50} = inhibitory concentration at 50%; TGF-β = transforming growth factor-beta.

cells (Fig 2A). Clonogenic assay also showed that TGF-β and EGF induced-EMT improved clonogenic survival in A549 cells (Fig 2A). Table 1 shows the IC_{50} values for cisplatin and paclitaxel in A549 cells with or without EMT induction.

EMT-Induced Cells Observed In Vitro After Exposure to Chemotherapy or Radiotherapy

A stable treatment-resistant phenotype was generated by chronic exposure of A549 cells to cisplatin, paclitaxel, or radiation. These sub-lines showed phenotypic changes such as a spindle-cell shape (Fig 2B). Table 1 shows the IC_{50} values for cisplatin and paclitaxel in parent A549 cells and drug resistance cells calculated by MTT assay. A proliferation assay showed improved clonogenic survival in each resistant sub-line (Fig 2C). The RT-PCR analysis also showed that the messenger (m)RNA level of E-cadherin was decreased, while the N-cadherin and vimentin mRNA levels were increased in the resistant cells (Fig 2D), indicating that acquisition of resistance to chemotherapy or radiation-induced molecular changes that were consistent with those induced by EMT.

Expression of EMT Markers in Clinical Samples

The characteristics of the 63 patients are shown in Table 2. Immunohistochemical staining was used to analyze the protein expressions of the epithelial markers E-cadherin and cytokeratin, and the mesenchymal markers N-cadherin and vimentin in tumor specimens. Representative immunohistochemical staining findings are shown in Figure 3. The epithelial markers were detected in nearly all biopsy specimens from patients with NSCLC before CRT whereas the mesenchymal markers were detected in 20 of 63 tumors. Tumors obtained from 13 of 63 patients showed complete response to induction CRT. While the tumor response to CRT was not significantly associated with the expression of mesenchymal markers, only 2 of the 13 tumors that achieved a complete response to CRT expressed mesenchymal proteins (Appendix 2). There was no difference in regard to DFS between patients with and without mesenchymal protein expression noted in specimens obtained before treatment (Fig 4A).

Given the results of the in vitro study, we hypothesized that preoperative CRT might induce EMT changes in tumor tissue and that these changes might be associated with a chemoresistance mechanism and poor prognosis. Thus, we compared protein expressions of the epithelial and mesenchymal markers in tumor specimens obtained both before and after CRT from patients with NSCLC. We excluded patients in whom the tumor was completely diminished after induction CRT and focused on the 50 remaining patients who showed an incomplete response to induction CRT (Table 3). While the mesenchymal

Table 2. Patient Characteristics (n = 63)

Characteristics	No. of Patients
Age	58 ± 10
Gender	
Male	56
Female	7
Clinical T status	
T1	2
T2	29
T3	17
T4	15
Clinical N status	
N0	6
N1	14
N2	41
N	32
Clinical stage	
2B	16
3A	31
3B	16
Histology	
Adenocarcinoma	27
Squamous cell carcinoma	30
Others	6
Pathologic stage	
0	13
1A–1B	16
2A–2B	12
3A	19
3B	3
Chemotherapy	
CDDP+VDS (+MMC)	38
CDDP+VNR	16
CDDP+Doce	9
Radiation (Gy)	43 ± 9.3
Surgical procedure	
Lobectomy	40
Pneumonectomy	23
With combined resection	
Bronchoplasty	8
Rib	5
Pericardium	4
Major vesse	12
Diaphragma	1

CDDP = cisplatin; Doce = docetaxel; MMC = mitomycin; VDS = vindesine; VNR = vinorelbine.

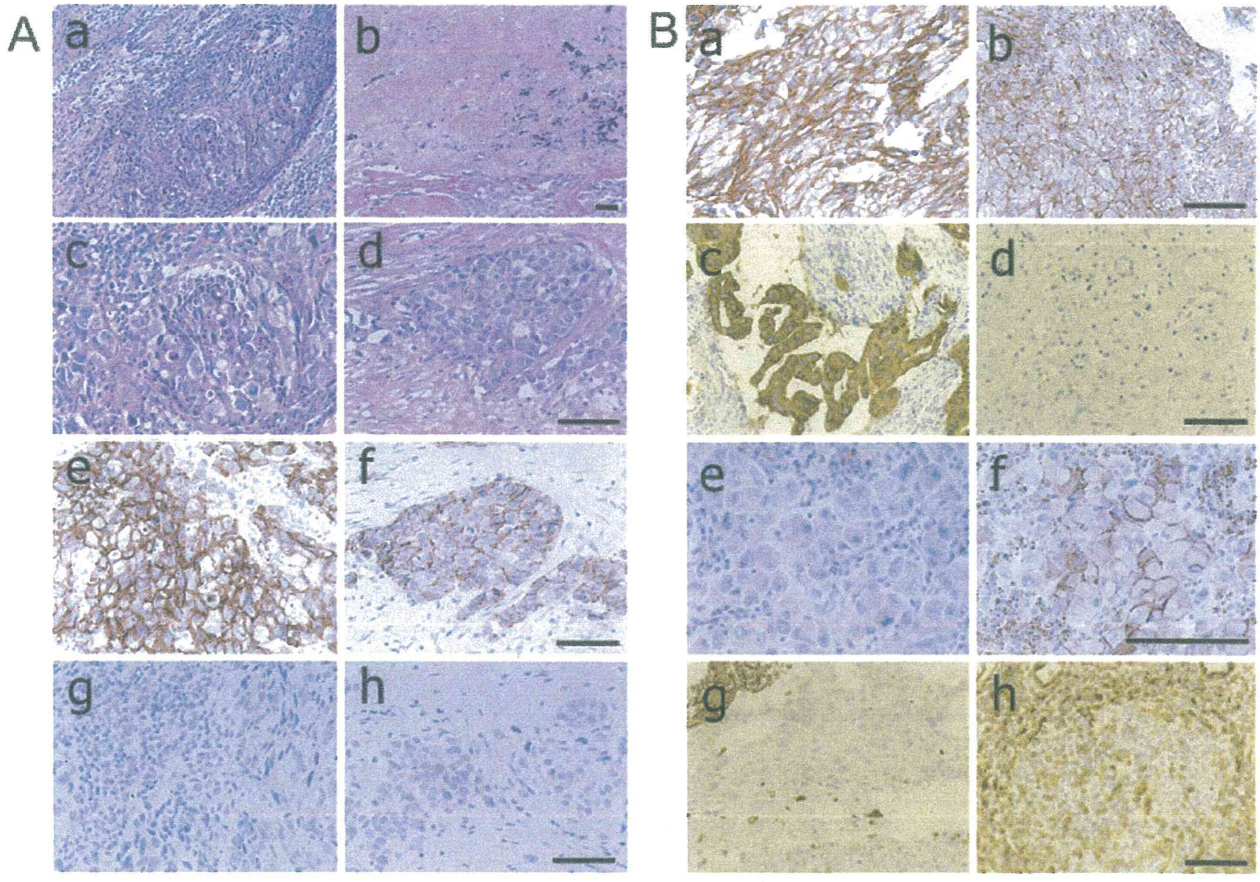

Fig 3. Immunohistochemical staining was used to analyze the protein expressions of E-cadherin and cytokeratin as epithelial markers and of N-cadherin and vimentin as mesenchymal markers in tumors before and after chemoradiotherapy (CRT) treatment. All sections were scored in a semiquantitative manner as described in the protocol noted in Materials and Methods and the staining grade was classified as 0 (score < 10), +1 (10≤, <30), +2 (30≤, <70), or +3 (70≤). (A) Panels a–h show representative findings from a patient who received induction CRT followed by surgery. a–d: hematoxylin & eosin staining; e, f: E-cadherin staining; g, h: N-cadherin staining; a, c, e, g: pre-CRT; b, d, f, h: post-CRT. (B) a, b: E-cadherin staining; c, d: cytokeratin staining, e, f: N-cadherin staining; g, h: vimentin staining; a, c, e, g: pre- CRT; b, d, f, h: post- CRT. Scale bar = 50 μm.

markers were detected in 21 of 50 tumors resected after CRT, these markers did not predict the DFS in patients with NSCLC (Fig 4B, $p = 0.239$). After CRT, expression of the epithelial markers was decreased in 15 of 50 surgically resected specimens (Table 4; Appendix 3). On the other hand, expression of the mesenchymal markers was increased after CRT in 15. In 10 of the specimens a decrease in epithelial markers and an increase in mesenchymal markers were detected, while at least one of these changes was detected in 10 specimens. Thus, a total of 20 specimens showed EMT-like changes in response to induction CRT. We classified patients with decreased epithelial markers or increased mesenchymal markers as the EMT marker-positive group (n = 20), and the others as the EMT negative group. According to a clinicopathologic comparison of these groups, the pathologic N status in the EMT marker-positive group was significantly lower than that in the EMT marker-negative group (Table 3). However, the DFS rate of patients in the EMT marker-positive group was significantly lower than that of patients in the EMT marker-negative group (Fig 4C). Five variables, including tumor response to CRT, pathologic nodal metastasis, operating procedure, histology, and EMT change, were analyzed using a Cox proportional hazards regression model to determine the variables having an effect on DFS in NSCLC patients. The univariate analyses revealed that tumor response to CRT and EMT change after CRT were related to DFS (Table 5). The multivariate analysis revealed that EMT change was an independent variable predicting DFS (Table 6).

Comment

We found that EMT leads to reduced sensitivity to chemotherapy in NSCLC cells, and that chronic exposure to chemotherapy or radiation transforms NSCLC cells into therapy-resistant sub-lines. Zhuo and colleagues [16, 17] reported that blocking EMT by knockdown of Snail or Twist, zinc finger transcription factors and key E-cadherin repressor molecules in the process of EMT,

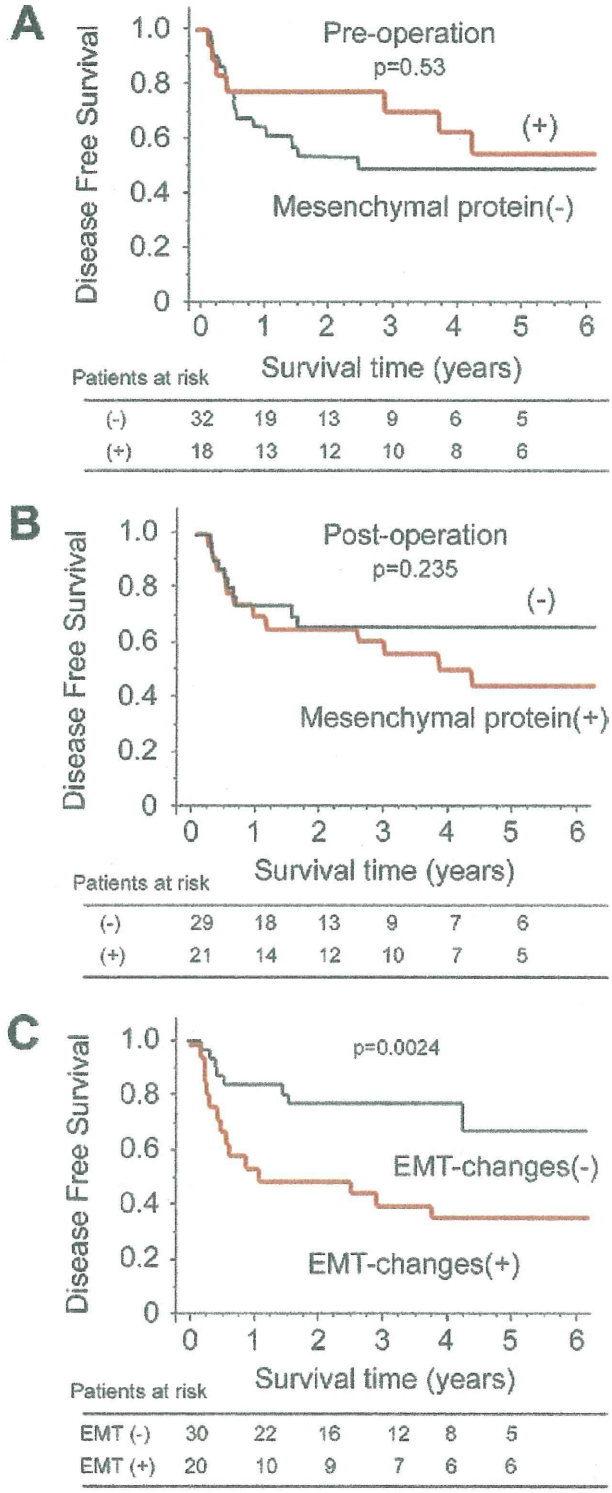

Fig 4. (A) Disease-free survival (DFS) rates according to tumor expression of mesenchymal markers before chemoradiotherapy (CRT). (B) The DFS rates according to tumor expression of mesenchymal markers after CRT. (C) The DFS rates according to EMT changes in response to CRT. The DFS rate of patients with epithelial to mesenchymal transition (EMT) changes such as decreased epithelial markers and increased mesenchymal markers as response to CRT was significantly lower than that of patients without EMT changes.

Table 3. Patient Characteristics (n = 50)

Variables	EMT-Changes After Chemoradiotherapy		
	EMT (−) (n = 30)	EMT (+) (n = 20)	*p* Value[a]
Age	59 ± 10	54 ± 10	0.039
Gender			
Male	26 (67%)	19 (95%)	0.336
Female	4 (13%)	1 (5%)	
Clinical T status			
1	0 (0%)	2 (10%)	
2	17 (57%)	8 (40%)	0.112
3	9 (30%)	4 (20%)	
4	4 (13%)	6 (30%)	
Clinical N status			
0	2 (7%)	3 (15%)	
1	7 (23%)	4 (20%)	0.787
2	20 (67%)	12 (60%)	
3	1 (3%)	1 (5%)	
Clinical stage			
2B	7 (23%)	5 (25%)	
3A	19 (63%)	8 (40%)	0.151
3B	4 (13%)	7 (35%)	
Histology			
Adenocarcinoma	11 (37%)	9 (45%)	
Squamous cell carcinoma	15 (50%)	10 (50%)	0.594
Others	4 (13%)	1 (5%)	
Chemotherapy			
CDDP+VDS (+MMC)	21 (70%)	13 (65%)	
CDDP+VNR	6 (20%)	3 (15%)	0.586
CDDP+Doce	3 (10%)	4 (20%)	
Radiation (Gy)	42 ± 10	45 ± 9.3	0.489
Surgical procedure			
Lobectomy	18 (60%)	12 (60%)	>0.999
Pneumonectomy	12 (40%)	8 (40%)	
Response to chemoradiotherapy			
Minor response	10 (33%)	4 (20%)	0.304
Major response	20 (67%)	16 (80%)	
Pathologic N status			
N0–1	16 (53%)	17 (85%)	0.021
N2	14 (47%)	3 (15%)	
Pathologic stage			
1A–1B	10 (33%)	9 (45%)	
2A–2B	5 (17%)	6 (30%)	0.195
3A–3B	15 (50%)	5 (25%)	

[a] $p = \chi^2$ test, or Mann-Whitney test.

CDDP = cisplatin; Doce = docetaxel; EMT = epithelial to mesenchymal transition; MMC = mitomycin; Response to chemoradiotherapy: Minor = more than two thirds cancer cells viable; Major = fewer than one third of cancer cells viable; VDS = vindesine; VNR = vinorelbine.

Table 4. Summary of Epithelial to Mesenchymal Transition (EMT) Status by Immunohistochemistry

EMT Markers	No. of Patients
Decrease of epithelial marker	15
E-cadherin (decrease)	14
Cytokeratin (decrease)	7
Increase mesenchymal marker	15
N-cadherin (increase)	11
Vimentin (increase)	8

increases the sensitivity of A549 cells to cisplatin. Those findings indicated that EMT is associated with acquired resistance to chemotherapy or radiotherapy in NSCLC. Furthermore, it has been reported that EMT negatively affects cellular response to EGFR-TKI (EGF receptor tyrosine kinase inhibitor) in vitro and in vivo [18]. In addition, EMT derived from repeated exposure to gefitinib, an EGFR-TKI, determines subsequent sensitivity to EGFR inhibitors as well as other anti-cancer drugs in A549 cells [23]. These data raise the possibility that an appropriate combination of CRT in an EMT-targeted strategy might be a promising approach for NSCLC therapy. Indeed, blocking EMT by restoration of E-cadherin has been shown to enhance the sensitivity to EGFR-TKI [24].

The concept of "cadherin switching" has been reported to be one of the key events in EMT in some kinds of cancer [8, 25]. Inactivation of E-cadherin is an important event in tumor progression [26, 27]. Activation of an inappropriate cadherin, such as N-cadherin, would be a subsequent event and might promote angiogenesis, brain metastasis, and poor survival [28, 29]. Basic studies have revealed interactions between N-cadherin and fibroblast growth factor receptor [30], which activates PI3K pathway signaling. Furthermore, we previously reported that stimulation of tumor stroma components induces EMT through a PI3K-extracellular signal-regulated kinases pathway [20].

Table 5. Univariate Analysis of Disease-Free Survival

Factors	Hazard Ratio	95% CI	*p* Value
Response to chemoradiotherapy			
Major versus minor	3.46	1.012–12.17	0.049
Nodal status			
pN2 vs pN0-1	1.27	0.53–3.00	0.594
Histology			
AD versus others	0.97	0.42–2.26	0.949
Surgical procedure			
Pneu versus lobe	1.10	0.47–2.57	0.831
EMT status			
EMT (+) vs (−)	3.15	1.33–7.47	0.0091

AD = adenocarcinoma; CI = confidence interval; EMT = epithelial to mesenchymal transition; lobe = lobectomy; Response to chemoradiotherapy: Minor = more than two thirds cancer cells viable; Major = fewer than one third of cancer cells viable; Pneu = pneumonectomy.

Table 6. Multivariate Analysis of Disease-Free Survival

Factors	Hazard Ratio	95% CI	*p* Value
Response to chemoradiotherapy			
Major vs minor	2.86	0.81–10.0	0.102
EMT status			
EMT (+) vs (–)	2.79	1.17–6.67	0.021

CI = confidence interval; EMT = epithelial to mesenchymal transition; Response to chemoradiotherapy: Minor = more than two thirds cancer cells viable; Major = fewer than one third of cancer cells viable.

These data suggested that survival signals in the EMT process might make cancer cells insensitive to chemoradiotherapy.

The immunohistochemistry study detected expression of mesenchymal proteins in specimens obtained from 20 of 63 patients who underwent preoperative CRT, indicating that some tumors might undergo EMT prior to treatment. Where the response to CRT was not significantly associated with the expression of mesenchymal proteins in the present study ($p = 0.067$), 2 of 12 tumors that achieved complete response to CRT expressed mesenchymal proteins, indicating that mesenchymal proteins could be biomarkers predicting response to induction CRT using biopsy specimens before treatment. In the in vitro study we investigated whether preoperative CRT might induce EMT changes in tumor tissues. A detailed study of the EMT status of NSCLC using matched specimens from both pretreatment and post-treatment is essential to investigate the association between EMT and resistance to chemotherapy or radiotherapy in patients with NSCLC. In this study we found that 20 specimens showed EMT-like changes in response to induction CRT. While the pathologic N status in the EMT marker-positive group was significantly lower than that in the EMT marker-negative group, the DFS rate of patients in the EMT marker-positive group was significantly lower than that of patients in the EMT marker-negative group. Furthermore, a Cox proportional hazards regression model revealed that the EMT-like change was an independent prognostic indicator of DFS. Thus, the changes in EMT markers induced in tumor specimens after CRT may be useful biomarkers in patients with NSCLC. We believe that the EMT change precisely indicates the malignant potential of NSCLC even in patients with down-staged disease.

In conclusion, EMT was shown to lead not only to increased malignancy potential, but also to reduced sensitivity to cisplatin, paclitaxel, and radiation in NSCLC cells. Chronic exposure to cisplatin, paclitaxel, or radiation altered NSCLC cells into therapy-resistant sub-lines. Furthermore, EMT marker expression was detected after CRT in tumors resected from patients with NSCLC. Thus, EMT may make NSCLC tumors insensitive to CRT. New therapeutic combinations using EMT-signaling inhibitors are expected to circumvent the resistance of cancers to CRT.

This work was supported by KAKENHI (Grants-in-Aid for Scientific Research) 22890106 and the Takeda Science Foundation.

References

1. Spira A, Ettinger DS. Multidisciplinary management of lung cancer. N Engl J Med 2004;350:379–92.
2. Carney DN. Lung cancer--time to move on from chemotherapy. N Engl J Med 2002;346:126–8.
3. Friedel G, Budach W, Dippon J, et al. Phase II trial of a trimodality regimen for stage III non-small-cell lung cancer using chemotherapy as induction treatment with concurrent hyperfractionated chemoradiation with carboplatin and paclitaxel followed by subsequent resection: a single-center study. J Clin Oncol 2010;28:942–8.
4. Weder W, Collaud S, Eberhardt WE, et al. Pneumonectomy is a valuable treatment option after neoadjuvant therapy for stage III non-small-cell lung cancer. J Thorac Cardiovasc Surg 2010;139:1424–30.
5. Bremnes RM, Veve R, Gabrielson E, et al. High-throughput tissue microarray analysis used to evaluate biology and prognostic significance of the E-cadherin pathway in non-small-cell lung cancer. J Clin Oncol 2002;20:2417–28.
6. Thiery JP. Epithelial-mesenchymal transitions in development and pathologies. Curr Opin Cell Biol 2003;15:740–6.
7. Wheelock MJ, Johnson KR. Cadherins as modulators of cellular phenotype. Annu Rev Cell Dev Biol 2003;19:207–35.
8. Wheelock MJ, Shintani Y, Maeda M, Fukumoto Y, Johnson KR. Cadherin switching. J Cell Sci. 2008;121(Pt 6):727–35.
9. Takeichi M. Cadherin cell adhesion receptors as a morphogenetic regulator. Science 1991;251:1451–5.
10. Liu D, Huang C, Kameyama K, et al. E-cadherin expression associated with differentiation and prognosis in patients with non-small cell lung cancer. Ann Thorac Surg 2001;71:949–54.
11. Nieman MT, Prudoff RS, Johnson KR, Wheelock MJ. N-cadherin promotes motility in human breast cancer cells regardless of their e-cadherin expression. J Cell Biol 1999;147:631–44.
12. Maeda M, Johnson KR, Wheelock MJ. Cadherin switching: Essential for behavioral but not morphological changes during an epithelium-to-mesenchyme transition. J Cell Sci 2005;118(Pt 5):873–87.
13. Bremnes RM, Veve R, Gabrielson E, et al. High-throughput tissue microarray analysis used to evaluate biology and prognostic significance of the E-cadherin pathway in non-small-cell lung cancer. J Clin Oncol 2002;20:2417–28.
14. Deeb G, Wang J, Ramnath N, et al. Altered E-cadherin and epidermal growth factor receptor expressions are associated with patient survival in lung cancer: a study utilizing high-density tissue microarray and immunohistochemistry. Mod Pathol 2004;17:430–9.
15. Soltermann A, Tischler V, Arbogast S, et al. Prognostic significance of epithelial-mesenchymal and mesenchymal-epithelial transition protein expression in non-small cell lung cancer. Clin Cancer Res 2008;14:7430–7.
16. Zhuo WL, Wang Y, Zhuo XL, Zhang YS, Chen ZT. Short interfering RNA directed against TWIST, a novel zinc finger transcription factor, increases A549 cell sensitivity to cisplatin via MAPK/mitochondrial pathway. Biochem Biophys Res Commun 2008;369:1098–102.
17. Zhuo W, Wang Y, Zhuo X, Zhang Y, Ao X, Chen Z. Knockdown of Snail, a novel zinc finger transcription factor, via RNA interference increases A549 cell sensitivity to cisplatin via JNK/mitochondrial pathway. Lung Cancer 2008;62:8–14.
18. Thomson S, Buck E, Petti F, et al. Epithelial to mesenchymal transition is a determinant of sensitivity of non-small-cell lung carcinoma cell lines and xenografts to epidermal growth factor receptor inhibition. Cancer Res 2005;65:9455–62.
19. Del Castillo G, Murillo MM, Alvarez-Barrientos A, et al. Autocrine production of TGF-beta confers resistance to apoptosis after an epithelial-mesenchymal transition process in hepatocytes: Role of EGF receptor ligands. Exp Cell Res 2006;312:2860–71.
20. Shintani Y, Maeda M, Chaika N, Johnson KR, Wheelock MJ. Collagen I promotes epithelial-to-mesenchymal transition in lung cancer cells via transforming growth factor-beta signaling. Am J Respir Cell Mol Biol 2008;38:95–104.
21. Bertolini G, Roz L, Perego P, et al. Highly tumorigenic lung cancer CD133+ cells display stem-like features and are spared by cisplatin treatment. Proc Natl Acad Sci U S A 2009;106:16281–6.
22. McCarty KS Jr, Szabo E, Flowers JL, et al. Use of a monoclonal anti-estrogen receptor antibody in the immunohistochemical evaluation of human tumors. Cancer Res 1986;46(8 Suppl):4244s–48s.
23. Rho JK, Choi YJ, Lee JK, et al. Epithelial to mesenchymal transition derived from repeated exposure to gefitinib determines the sensitivity to EGFR inhibitors in A549, a non-small cell lung cancer cell line. Lung Cancer 2009;63:219–26.
24. Witta SE, Gemmill RM, Hirsch FR, et al. Restoring E-cadherin expression increases sensitivity to epidermal growth factor receptor inhibitors in lung cancer cell lines. Cancer Res 2006;66:944–50.
25. Cavallaro U, Schaffhauser B, Christofori G. Cadherins and the tumour progression: is it all in a switch? Cancer Lett 2002;176:123–8.
26. Nakashima T, Huang C, Liu D, et al. Neural-cadherin expression associated with angiogenesis in non-small-cell lung cancer patients. Br J Cancer 2003;88:1727–33.
27. Saad AG, Yeap BY, Thunnissen FB, et al. Immunohistochemical markers associated with brain metastases in patients with nonsmall cell lung carcinoma. Cancer 2008;113:2129–38.
28. Prudkin L, Liu DD, Ozburn NC, et al. Epithelial-to-mesenchymal transition in the development and progression of adenocarcinoma and squamous cell carcinoma of the lung. Mod Pathol. 2009;22:668–78.
29. Grinberg-Rashi H, Ofek E, Perelman M, et al. The expression of three genes in primary non-small cell lung cancer is associated with metastatic spread to the brain. Clin Cancer Res 2009;15:1755–61.
30. Suyama K, Shapiro I, Guttman M, Hazan RB. A signaling pathway leading to metastasis is controlled by N-cadherin and the FGF receptor. Cancer Cell 2002;2:301–14.

Appendix 1. List of Antibodies and Other Reagents Used in This Study

Antibodies	Clone	Company	Application
Anti-E-cadherin mouse mAb	HECD-1	Takara, Shiga, Japan	IF
Anti-E-cadherin mouse mAb	NCH-38	Dako, Carpinteria, CA	IHC
Anti-N-cadherin mouse mAb	8C11	Abcam, Cambridge, MA	IF
Anti-N-cadherin mouse mAb	6G11	Dako, Carpinteria, CA	IHC
Anti-cytokeratin mouse mAb	AE1/AE3	Dako, Carpinteria, CA	IHC
Anti-vimentin mouse mAb	V9	Sigma, St. Louis, MO	IHC
Reagents			
Cisplatin		Sigma, St. Louis, MO	
Paclitaxel		Sigma, St. Louis, MO	
EGF		Sigma, St. Louis, MO	
TGF-β1		R&D Systems, Minneapolis, MO	
TaqMan assays			
E-cadherin, Hs00170423_m1			AppliedBiosystems
N-cadherin, Hs00169953_m1			

IF = immunofluorescence; IHC = immunohistochemistry.

Appendix 2. Preoperative EMT Status and Response to Chemoradiotherapy

Response to Chemoradiotherapy	Expression of Mesenchymal Proteins		
	EMT (−)	EMT (+)	p Value[a]
Complete	11	2	0.155
Non-complete	32	18	

[a] p value from the χ^2 test.

EMT = epithelial to mesenchymal transition.

Appendix 3. Expression Changes of the Epithelial Markers and Mesenchymal (EMT) Markers Before and After Chemoradiotherapy

A. Expression of E-cadherin

	Post-chemoradiotherapy			
Pre-chemoradiotherapy	0	1+	2+	3+
0	0	0	0	0
1+	1	2	0	0
2+	1	0	0	0
3+	1	5	4	36

B. Expression of cytokeratin

	Post-chemoradiotherapy			
Pre-chemoradiotherapy	0	1+	2+	3+
0	1	0	0	0
1+	0	1	0	0
2+	0	1	0	1
3+	1	2	3	40

C. Expression of N-cadherin

	Post-chemoradiotherapy			
Pre-chemoradiotherapy	0	1+	2+	3+
0	33	8	0	0
1+	1	4	3	0
2+	0	0	0	0
3+	1	0	0	0

D. Expression of vimentin

	Post-chemoradiotherapy			
Pre-chemoradiotherapy	0	1+	2+	3+
0	33	3	0	0
1+	0	4	4	0
2+	0	1	1	1
3+	1	0	0	3

Changes in EMT status are indicated in bold.

DISCUSSION

DR ROSS M. BREMNER (Phoenix, AZ): You concentrate a lot on just the cancer cells themselves and the EMT [epithelial to mesenchymal transition] of the cancer cells. Can you give us your thoughts on what EMT from the stroma might be playing a role in this pre- and post-chemoradiation?

DR SHINTANI: We can see massive fibrotic area after induction chemotherapy. And as you said, we found many fibroblasts in the stroma tissues, but we did not see the EMT markers for the stroma cells. But now we have focused on the cancer associated with fibroblasts because these fibroblasts are producing many growth factors. So these fibroblasts may be the target of the cancer therapy in the future.

DR BREMNER: Thank you.

DR ALYKHAN S. NAGJI (Charlottesville, VA): The cell line that you used was an adenocarcinoma cell line. Did you find anything in the squamous cell lines, and what were the histologies of the tissues that you used?

DR SHINTANI: Your question is whether we used other cells, such as squamous cells?

DR NAGJI: Other cell lines, squamous cell. And then the histology of the tissue samples that you used, were those adenocarcinoma or squamous cell carcinoma?

DR SHINTANI: Yes. We showed only adenocarcinoma cell lines, but we used another large cell carcinoma or the squamous cell carcinoma cells.

And the last part of my talk is using human tissues and we can also see these EMT changes in the squamous cell carcinoma after induction chemoradiotherapy.

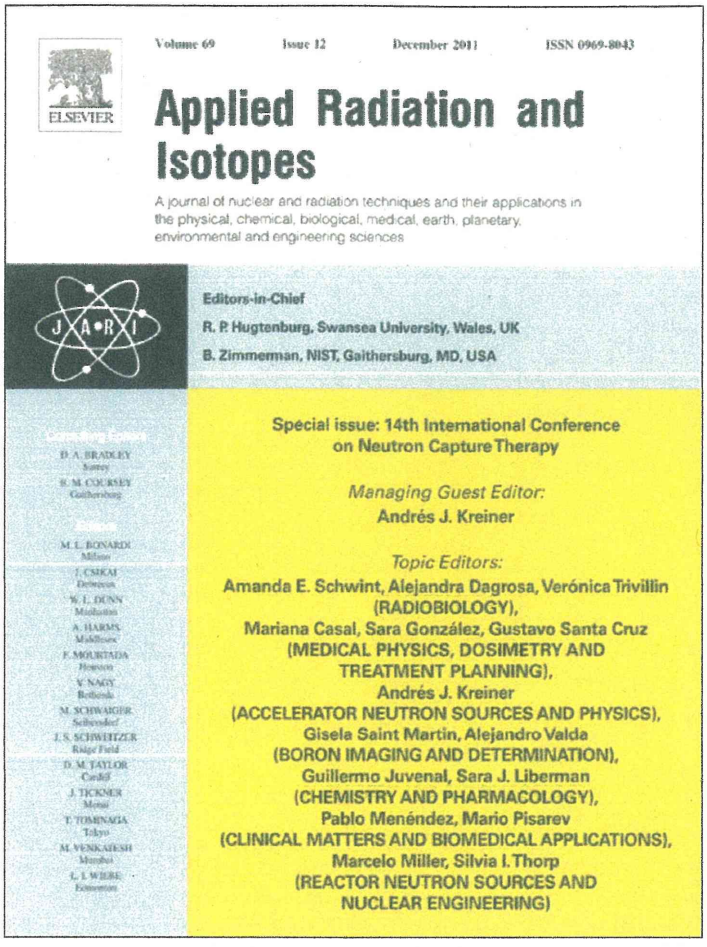

Applied Radiation and Isotopes 69 (2011) 1768–1770

Contents lists available at ScienceDirect

Applied Radiation and Isotopes

journal homepage: www.elsevier.com/locate/apradiso

Synthesis of optically active dodecaborate-containing L-amino acids for BNCT

Shintaro Kusaka [a], Yoshihide Hattori [a,*], Kouki Uehara [b], Tomoyuki Asano [b], Shinji Tanimori [a], Mitsunori Kirihata [a]

[a] Department of Bioscience and Informatics, Graduate School of Life and Environmental Sciences, Osaka Prefecture University, 1-1 Gakuen-cho, Nakaku, Sakai, Japan
[b] Stella Pharma Corporation, ORIX Kouraibashi Bldg. 5F 3-2-7 Kouraibashi, Chuo-ku, Osaka, Japan

ARTICLE INFO

Available online 8 April 2011

Keywords:
Boron cluster containing L-α-amino acid
Dodecaboratethio-L-amino acid
New boron amino acid for BNCT

ABSTRACT

A convenient and simple synthetic method of dodecaboratethio-L-amino acid, a new class of tumor-seeking boron carrier for BNCT, was accomplished from *S*-cyanoethylthioundecahydro-*closo*-dodecaborate (*S*-cyanoethyl-^{10}BSH, $[^{10}B_{12}H_{11}]^{2-}SCH_2CH_2CN$) and bromo-L-α-amino acids by nearly one step *S*-alkylation. An improved synthesis of *S*-cyanoethyl-^{10}BSH, a key starting compound for *S*-alkylation, was also performed by Michael addition of ^{10}BSH with acryronitrile in high yield. Four kinds of new dodecaboratethio-L-amino acids were obtained in optically pure form without the need for any optical resolution.

1. Introduction

Boron-containing L-amino acids are worthwhile synthetic targets due to their potential biological activities, particularly with respect to the boron-neutron capture therapy (BNCT). In many tumor tissues, L-amino acid transport is enhanced to guarantee the multiplication of tumor cells compared with normal tissues (Endou and Kanai, 1999). Therefore, various boron-containing α-amino acids that are closely similar in structure to the usual amino acid such as *p*-boronophenylalanine (BPA) and *o*-carboranyl-glycine, have been synthesized and evaluated (Varadarajan and Hawthorne, 1991; Srivastsva et al., 1997). However, such boron-containing amino acids have low water-solubility associated with poor bioavailability as disadvantages.

Recently, Gabel et al. reported that the synthesis of a new class of water soluble α-amino acids in racemic states, which contained the dianionic dodecaboratethio ($[^{10}B_{12}H_{11}]^{2-}$-S-) unit from undecahydro-*closo*-dodecaborate (BSH) by stepwise alkylation using bromoalkyl-*N*-aceto-amidomalonate derivatives followed by decarboxylation and hydrolytic deprotection (Slepukhina and Gabel, 2006). However, these methods have not been entirely satisfactory, particularly for large amount preparation owing to multiple steps, and for racemic form of the target amino acids.

Here, we describe an efficient route for the simple synthesis of optically pure dodecaboratethio-L-amino acids **1–4** (Fig. 1) as illustrated in the schemes.

2. Material and method

2.1. General

^{1}H NMR spectra were measured on a JMTC-400/54/SS (400 MHz, JEOL Ltd., Tokyo, Japan) spectrometer. The chemical shifts in ^{1}H NMR are given in δ values from TMS used as internal standard. Optical rotations were measured on a Jasco P-2200 polarimeter (JASCO Co., Tokyo, Japan). Electron spray ionization time of flight mass spectra (ESI-TOF MS) was obtained on a Nanofrontier LD (Hitachi High-Technologies Corporation, Tokyo, Japan). ^{10}BSH was provided by Stella Pharma Corporation (Osaka, Japan).

2.2. Synthesis of bis-tetramethylammmonium S-(cyanoethyl)-thioundecahydro-closo-dodecaborate (2) by Michael addition

To a solution of ^{10}BSH.2NMe$_4$ (1.00 g, 3.20 mmol) and 1N NaOH aq. (3.20 mL, 3.20 mmol) in H_2O (20 mL) was added acrylonitrile (255 mg, 4.80 mmol) at room temperature. After stirring for 3 h, the reaction mixture was washed with EtOAc (20 mL × 3), and the aqueous layer was concentrated in vacuo. The residual solid was recrystallized from H_2O to give **2** as colorless crystal (1.08 g, 92%): mp 280–285 °C, ^{1}H NMR (400 MHz, D_2O) δ 0.7–1.5 (11H, m, $^{10}B_{12}H_{11}$), 2.56 (2H, m, $CNCH_2CH_2S$-), 2.65 (2H, m, $CNCH_2CH_2S$-), 3.10 (24H, s, $-N^+(CH_3)_4$).

2.3. Synthesis of dodecaboratethio-L-amino acids (1a–d)

The mixture of bis-tetramethylammmonium *S*-(cyanoethyl)thio-undecahydro-*closo*-dodecaborate (**2**, 0.27 mmol) and ω-bromo-L-amino acids **3a–d** (0.41 mmol) in dry MeCN (7 mL) under argon atmosphere was refluxed for 12 h, and the reaction mixture was

* Corresponding author.
E-mail address: y0shi_hattori@riast.osakafu-u.ac.jp (Y. Hattori).

0969-8043/$ - see front matter © 2011 Elsevier Ltd. All rights reserved.
doi:10.1016/j.apradiso.2011.03.042

concentrated in vacuo. The residual solid was suspended in acetone (30 mL), and the suspension was filtrated by suction to remove the insoluble solid. To the filtrate was added 10% tetramethylammonium hydroxide in MeOH (0.28 mmol) at 0 °C, and the mixture was stirred for 30 min at the same temperature. The collected precipitate by filtration was washed quickly with acetone (30 mL). After dissolving with water, the aqueous solution was passed through an ion-exchange column (Amberlite IR-120, H^+ form). The neutralized filtrate with NaOH was chromatographed using of ODS column to give pure dodecaboratelthio-L-amino acids **1a–d**.

2.3.1. (R)-2-Amino-3-(dodecaboranylthio)pro-panoic acid disodium salt (1a)

^{1}H NMR (D_2O); 0.75–1.80 (11H, m, $^{10}B_{12}H_{11}$), 2.52–2.66 (2H, m, 3-CH_2), 3.80 (1H, m, 2-CH); ESI-TOF MS (neg.): found m/z 274.5 $[M+Na]^-$ (calcd. for $C_3H_{17}^{10}B_{12}NO_2S$+Na: 274.2).

2.3.2. (S)-2-Amino-4-(dodecaboranylthio)butyric acid disodium salt (1b)

^{1}H NMR (D_2O); 0.75–1.60 (11H, m, $^{10}B_{12}H_{11}$), 1.91–2.03 (2H, m, 3-CH_2), 2.43 (2H, m, 4-CH_2), 3.62 (1H, m, 2-CH); $[\alpha]_D^{25}$ −1.93 (*c* 0.505, H_2O); ESI-TOF MS (neg.): found m/z 288.2 $[M+Na]^-$ (calcd. for $C_4H_{19}{}^{10}B_{12}NO_2S$+Na: 288.3).

2.3.3. (S)-2-Amino-5-(dodecaboranylthio)pentanoic acid disodium salt (1c)

^{1}H NMR (D_2O); 0.75–1.50 (11H, m, $^{10}B_{12}H_{11}$), 1.50 (2H, m, 4-CH_2), 1.60–1.80 (2H, m, 3-CH_2), 2.37 (2H, m, 5-CH_2), 3.30 (1H, m, 2-CH); $[\alpha]_D^{25}$ −2.06 (*c* 0.515, H_2O); ESI-TOF MS (neg.): found m/z 302.6 $[M+Na]^-$ (calcd. for $C_5H_{21}{}^{10}B_{12}NO_2S$+Na: 302.3).

2.3.4. (S)-2-Amino-5-(dodecaboranylthio)oc-tanoic acid disodiumsalt (1d)

^{1}H NMR (D_2O); 0.75–1.60 (11H, m, $^{10}B_{12}H_{11}$), 1.21–1.41(4H, m, 4-CH_2, 5-CH_2), 1.41 (2H, m, -6-CH_2), 1.70(4H, m, 3-CH_2-, 7-CH_2), 2.34 (2H, t, J=7.3 Hz, 8-CH_2), 3.57(1H, m, 2-CH); $[\alpha]_D^{25}$ −1.96 (*c* 0.515, H_2O); ESI-TOF MS (neg.): found m/z 344.5 $[M+Na]^-$ (calcd. for $C_8H_{27}{}^{10}B_{12}NO_2S$+Na: 344.3).

3. Results and discussion

In our initial attempt we employed direct alkylation of ^{10}BSH with ω-bromo-L-amino acid to prepare mono-*S*-alkyl^{10}BSH, however, the inseparable mixture of mono- and di-*S*-alkyl adducts were invariably formed. After several unsuccessful trials, we employed stepwise alkylation method using *S*-cyanoethyl-^{10}BSH (**2**), a key intermediate in this synthesis, according to the reported method (Gabel et al., 1993).

Gabel et al. have reported the stepwise synthesis of *S*-cyanoethyl-^{10}BSH (**2**), a useful intermediate for alkylation, stating from ^{10}BSH and bromo-propionitrile by two steps sequence. However, the overall yields were unsatisfactory.

We devised more efficient synthetic route based on hetero Michael reaction as shown in Scheme 1–3. Thus, ^{10}BSH was treated with acrylonitrile in aqueous solution using sodium hydroxide as a base to give pure *S*-cyanoethyl-^{10}BSH (**2**) as solid in 88% yields.

On the other hand, ω-bromo-L-amino acids (**3a–d**), represented as Br-(CH_2)n-CH(NH_2)COOH (n=1, 2, 3, 6), were prepared as hydrochloric or hydrobromic salts. Among them, (*S*)-2-amino-4-bromobutyric acid (**3b**, n=2) was commercially purchased, and other ω-bromo-L-amino acids bearing (*L*)-configuration were obtained

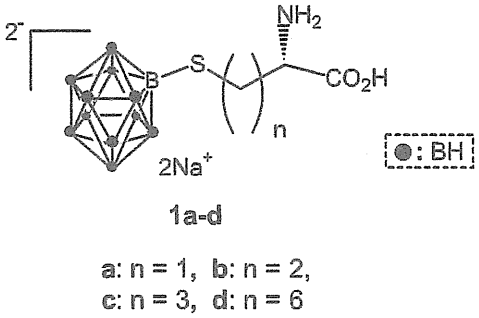

Fig. 1. Dodecaboratethio-L-amino acids.

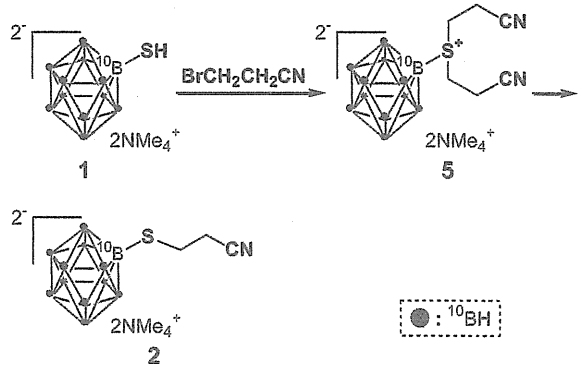

Scheme 2. Stepwise synthesis of *S*-cyanoethyl BSH by alkylation.

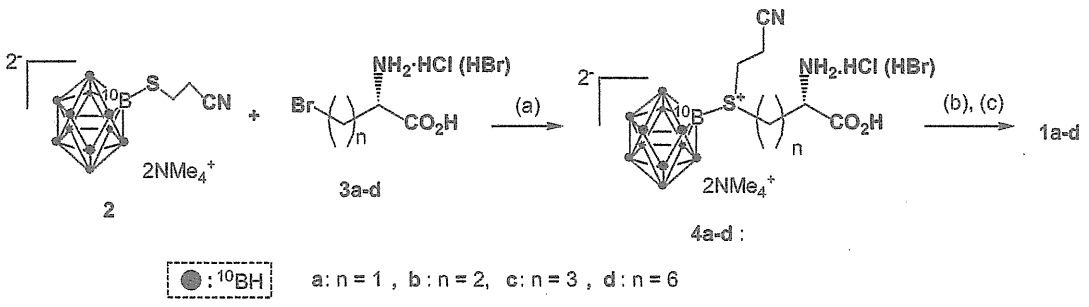

Reagents and conditions: a) MeCN, reflux, 24h, b) Me_4NOH, $MeNH_2$, acetone, r.t., 30 min, c) amberlite IR-120 (Na^+)

Scheme 1. Simple and efficient synthesis of dodecaboratethio -L-amino acids (**1a–d**).

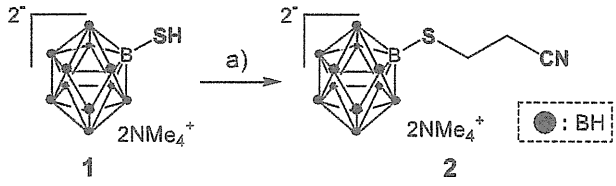

Reagents and conditions: a) acrylonitrile, NaOH / H_2O

Scheme 3. One step synthesis of *S*-cyanoethyl BSH by hetero Michael reaction.

according to the modified literature methods (Phadnis and Mugesh, 2005; Kanai et al., 1985; Watanabe et al., 2004), respectively.

General synthetic procedure for alkylation of **2** with bromo-L-amino acids (**3**) is very simple as follows; a mixture of **2** and **3** in acetonitrile was refluxed for one day, followed by condensation to give conjugates (**4**), which was used to the next step without further purification. Treatment of **4** in acetone with tetramethylammonium hydroxide (Me_4NOH) in the presence of methylamine furnished the target amino acid (**1**) in moderate yields. In the case of **1a**, the overall yields were poor (21%) due to its lability. The purity and chemical structure of **1** were analyzed by NMR, ESI-MS and capillary electrophoresis.

The biological activities of synthesized L-amino acids **1b–d** are currently examined using cultivated tumor cells and animals bearing B16 cancer cells.

4. Conclusions

We have accomplished the effective and simple synthesis of dodecaboratethio-L-amino acid by nearly one-step alkylation of *S*-cyanoethyl BSH, with non-protected bromo-L-amino acids in moderate yields. In the present synthesis, an absolute configuration of the starting bromo-L-amino acid is to be introduced to the final amino acids in retention. We believe that this synthetic method could be applied to another boron cluster containing optically active amino acids, such studies being currently progress. Biological study of the compounds obtained here is also now under investigation.

Acknowledgments

A part of this study is the result of "Studies on advanced boron neutron capture therapy using accelerator-based neutron source" carried out under the Strategic Promotion Program for Basic Nuclear Research by the Ministry of Education, Culture, Sports, Science and Technology of Japan.

References

Endou, H., Kanai, Y., 1999. Amino acid transporter molecule as a drug target. Nippon Yakugaku Zasshi 114, 11–16.

Gabel, D., Moller, D., Harfst, S., Rosler, J., Ketz, H., 1993. Synthesis of *S*-alkyl and *S*-acyl derivatives of mercaptoundecahydrododeca-borate, a possible boron carrier for neutron capture therapy. Inorg. Chem. 32, 2276–2278.

Kanai, F., Isshiki, K., Umezawa, Y., Morishima, H., Naganawa, H., Takita, T., Takeuchi, T., Umezawa, H., 1985. Vanoxonin, a new inhibitor of thymidylate synthetase. J. Antibiot. 38, 31–38.

Phadnis, P.P., Mugesh, G., 2005. Internally stabilized selenocysteine derivatives: syntheses, ^{77}Se NMR and biomimetic studies. Org. Biomol. Chem. 3, 2476–2481.

Srivastsva, R.R., Shinghaus, R.R., Kabalka, G.W., 1997. Synthesis of 1-amino-3-[2-(1,7-dicarba-*closo*-dodecaboran(12)-1-yl)ethyl]cyclo-butanecarboxylic acid. A Potential BNCT Agent 62, 4476–4478.

Slepukhina I., Gabel D., 2006. Synthesis and in vitro toxicity of new dodecaborate-containing amino acids, In: Proceedings of the 12th International Congress on Neutron Capture Therapy, pp. 247–250.

Varadarajan, A., Hawthorne, M.F., 1991. Novel carboranyl amino acids and peptides: reagents for antibody modification and subsequent neutron-capture studies. Bioconjugate Chem. 2, 242–253.

Watanabe, L.A., Jose, B., Kato, T., Nishino, N., Yoshida, M., 2004. Synthesis of L-α-amino-ω-bromoalkanoic acid for side chain modification. Tetrahedron Lett. 45, 491–494.